CHALMERS
UNIVERSITY OF TECHNOLOGY

Characterisation of solid flux in packed-fluidized bed:

Mixing response of a pulse input during fluidization

Master's thesis in Energy division

Mårten Bengtsson

DEPARTMENT OF SPACE, EARTH AND ENVIRONMENT
CHALMERS UNIVERSITY OF TECHNOLOGY
Gothenburg, Sweden 2022
www.chalmers.se

Master's thesis 2022

Characterisation of solid flux in packed-fluidized bed:

Mixing response of a pulse input during fluidization

MÅRTEN BENGTSSON

CHALMERS
UNIVERSITY OF TECHNOLOGY

Department of Space, Earth and Environment
Division of Energy Technology
Chalmers University of Technology
Gothenburg, Sweden 2022

Characterisation of solid flux in packed-fluidized bed:
Mixing response of a pulse input during fluidization
MÅRTEN BENGTSSON

Supervisor: Nasrin Nemati, Department of Space,Earth and Environment
Examiner: Magnus Rydén, Department of Space,Earth and Environment

Master's Thesis 2022
Department of Space,Earth and Environment
Division of Energy Technology
Chalmers University of Technology
SE-412 96 Gothenburg
Telephone +46 31 772 1000

Cover: The experiment setup at Chalmers is shown in the following image.

Typeset in LaTeX
Printed by Chalmers Reproservice
Gothenburg, Sweden 2022

Characterization of solid flux in packed-fluidized bed:
Mixing response of a pulse input during fluidization
Mårten Bengtsson
Department of Space,Earth and Environment
Chalmers University of Technology

Abstract

Fluidized beds have been around for more than 100 years and new applications are constantly developed. One of them, chemical looping combustion technique(CLC), works by letting the fuel react with fluidized solid oxygen carrier instead of air. Previous work have shown that CLC can produce combustion conditions with pure CO_2 flue gas stream [1], which would be more cost effective to pressurize and store compared to flue gas stream from air-combustion. One of the drawbacks of CLC is poor gas-mass transfer and the fluidized bed inability to achieve counter-current flow[1]. One approach that has shown improvement on the mass transfer is to introduce packing material to the fluidized bed to facilitate counter-current flow. Earlier work has shown packing material in the fluidized bed greatly increased the conversion of fuel to CO_2 in CLC applications.

This study investigated the potential of generating counter-current flow patterns for packed-fluidized bed, which can allow for reactor designs with better performance than thermodynamic equilibrium. To investigate the mixing response, a laboratory-scale cylindrical tubular reactor with dimensions 1 m high and 12 cm in diameter was used. Olivin sand with a diameter of 250-300 µm was used as bed material. The bed was fluidized with no packing material as a reference and the experiment were done with ASB 25.4 mm and ASB 6.35 mm as packing materials, at a 2-2.5:1 ratio packing to bed height, with a bed height of 20 cm. A magnetic tracer, magnetite of size 180-212 µm, together with magnetic sensors placed 13(outlet) and 47(inlet) cm from the the distributor plate were used to investigate the degree of plug flow using a pulse input method.

Pressure drop over the reactor was measured with 4 sensors, 13.2, 7.6 and 2.1 cm from the bottom. One was placed in the windbox before the distribution plate as reference. The bed was fluidized at superficial gas velocity of 0.1 and 0.3 m/s. Experiments were repeated three times per setup expect for when superficial gas velocity was 0.1 m/s and there was no packing in the bed. This due to insufficient fluidization.

Introducing packing material ASB 2.54 mm increased the degree of plug flow for both velocities, high velocity of 0.3 m/s showed higher degree of plug flow compared to 0.1 for the packing material ASB 25.4 mm. ASB 6.35 mm was too small and blocked the outlet yielding no plug flow or meaningful results. Using packed-fluidized bed increase the potential for plug flow and potential for efficient counter-current flow for fluidized bed. More work has to be done to further investigate the effect of confined beds on counter-current flow patterns.

Keywords: packed-fluidized bed,tracer, pulse input, fluidized bed

Acknowledgments

The author gratefully acknowledge the help of his supervisor Nasrin Nemati for being immensely helpful in the process. This thesis would not have been possible without out her help. The author is thankful for knowledge and input from his examiner Magnus Rydén.

Mårten Bengtsson, Gothenburg, June 2022

Contents

1 Introduction **1**
- 1.1 Background . . . 1
- 1.2 Aim . . . 2

2 Theory **3**
- 2.1 Fluidized beds . . . 3
- 2.2 Packed-fluidized bed . . . 5
- 2.3 Plug flow and tracer method . . . 6
- 2.4 Dispersion model . . . 9
- 2.5 Bulk Density . . . 10

3 Methods **11**
- 3.1 Experimental Setup . . . 11
  - 3.1.1 Reactor . . . 11
- 3.2 Preparation . . . 14
  - 3.2.1 Bed material . . . 14
  - 3.2.2 Calculating bulk density and particle size for inert and tracer . 15
  - 3.2.3 Void factor of packing materials . . . 15
  - 3.2.4 Packing and packing heights chosen . . . 16
  - 3.2.5 Flow rate . . . 17
- 3.3 Experimental Procedure . . . 17

4 Results **19**
- 4.1 Packing material ASB 25.4 mm . . . 19
- 4.2 Manual Sampling . . . 22
- 4.3 Dispersion model . . . 23

5 Discussion **25**
- 5.1 Influence of packing on plug flow in fluidized bed . . . 25
- 5.2 Error and limitations . . . 26

6 Conclusion **27**

References **27**

A Appendix 1 **I**
- A.1 Bulk density calculations . . . I

A.2 MATLAB I

1
Introduction

1.1 Background

Fluidized bed technology have been around for around 100 years and research is still being made to increase the efficiency and adaptability of fluidization applications. In 2008 the total installed capacity of fluidized bed combustion(FBC) was 30 GW_e [2].

Fluidized beds are devices where a two-phase continuum of solid particles and a fluid are made to behave similarly to a liquid, by means of a fluid stream. In a typical application, gas is injected from underneath the bed, through a distributor plate. The plate usually consist of a metal mesh with holes with a diameter smaller than the solid particles. The bed becomes fluidized when the gas that flows through start exerting a high enough friction force upwards to overcome the weight of the particles due to gravity.

One common applications for fluidized beds is combustion process, however drying, coating or adsorption have also adapted fluidized bed technology[3]. The key advantages of using fluidized bed devices for combustion processes are that subpar fuel can be burned at a large scale. Valmet has shown that this is possible when using a circulating fluidized bed(CFB) where the fluidizing bed acts as a heat distributor, allowing the fuel to burn more efficiently and emitting fewer harmful emissions such as nitrogen oxides [4]. Sumitomo also uses CFB for their combustion processes.

The world needs to rapidly reduce greenhouse gas emissions, mainly carbon dioxide(CO_2). Carbon capture and storage (CCS) has received a lot of attention as a key technology for achieving net zero emissions. One method of capturing carbon dioxide is to extract it directly from the flue gases of the combustion processes; however, this method has its drawbacks. Because air is used as the oxidizer, the flue gases will contain nitrogen gas, excess oxygen, CO_2, and water vapor. Capturing CO_2 from such flue gases requires a significant amount of energy, which reduces the efficiency of the entire combustion process. [5].

A novel approach to the problem is to let the fuel react with an oxygen carrier(ilmenite ore for example) instead of oxygen in the air. This can be done by using two internally connected reactors, called chemical-looping combustion(CLC). In the first reactor(fuel reactor), fuel and a fluidized oxygen carrier react to form heat and CO_2. After reacting with the fuel, the oxygen carrier has lost its oxygen and is transferred to the second reactor, known as the air reactor. The oxygen carrier absorbs oxygen and returns it to the fuel reactor, and the whole process can be

repeated. The key concept of CLC is that the process produces one stream with high concentration of CO_2 and one stream with mostly air. Leading to cheaper and more efficient carbon capture since no further extra energy is required in order to obtain pure CO_2 after combustion. An advantage compared to post combustion capture and storage.

One issue with CLC is that at a commercial scale, the process is limited by the mass transfer between the bubble and solid phases. The limitation originates from the growth of bubbles, rather than the reactivity of the gas and solid. Jesper Aronsson et al. have shown that introducing packing material to the fuel reactor greatly increased conversion rate of fuel to CO_2 [1]. According to Aronsson, this improvement was due to the effect of packings preventing the growth of bubbles, resulting in higher mass transfer between the bubble and solid phases. However; more research has to be made on the study of mass transfer between gases and solids, particularly when confide bed technology is utilized in conjunction with CLC.

In the general case, fluidized bed act as a simple stirred reactor where the bed material is perfectly mixed. If packing material is introduced to the reactor counter-current flow could be achieved with respect to solid and gas phases. Counter-current flow is common in the industry, particularly in heat exchangers. Two flows with different properties can effectively exchange properties, be it mass, heat or chemical with each other when utilizing counter-current flow.
Counter-current flow setups allows for an almost constant gradient(difference) between properties, meaning a higher driving force for exchanging properties. Other type of flows such as co-current(parallel) flow can, in the best case, exchange fifty percent of their properties before meeting thermodynamic equilibrium. For example in an equilibrium reaction where reactants react to form product, counter-current flow would push the equilibrium towards more product. Pablo Moreno has shown in his thesis that packed-fluidized bed can facilitate cross flow in the reactor.[6]. This work will investigate if counter-current flow can be achieved in a packed-fluidized bed. If this could be achieved, it would allow for better reactor designs and potential for CLC with better performance than thermodynamic equilibrium.

1.2 Aim

The purpose of this study is to determine whether solids plug flow is possible in a packed-fluidized bed, utilizing a pulse input of a tracer to study the mixing response. Investigating the differences between automatic and manual sampling in order to determine which technique is superior is a secondary goal.

2
Theory

In this chapter the overall theory of the work is presented.

2.1 Fluidized beds

Fluidized bed are, as mentioned in section 1, devices where solid particles are suspended by a fluid flowing upwards. The solid particles are collectively called the bed and the fluid can be either a gas or a liquid. The fluid is injected from underneath the bed, through a distributor plate. If the fluid has a low velocity the friction force that it exert on the bed of particles will not be enough to overcome the force of gravity on the particles. Instead it flows through the void between the bed of particles, this state is referred to a fixed bed. Increasing the flow rate of the fluid until the friction force equals the gravitational force transforms the bed into a fluidized bed, which is distinguished by the bed being fully suspended by the fluid. The bed is at this point fluidized and the bed of solid particles starts to behave as a liquid. Increasing the superficial gas velocity further results in bubbles formation, the system is at this point known as bubbling fluidized bed. Bubbling fluidized beds are more commonly used for gas-solid systems, the bubbles coalesce and grow as they progress further up the bed. The bed is a two phase system with respect to different solid particles concentration, known as bubble and emulsion phases. The bubble phase will have low amount of solid particles in it, less than one percent by volume[7]. The emulsion phase is characterized by high concentration of solid particles.

If the superficial gas velocity is increased further, a phenomena called slugging can start to occur. When slugging occurs the bubble diameter becomes equal or larger than the diameter of the reactor. The mass transfer in the slugging regime is lower than in bubbling fluidized bed regime. Figure 2.1 shows the different regime for a fluidized bed. The bed height increases as the bed becomes more fluidized by the increase in gas flow.

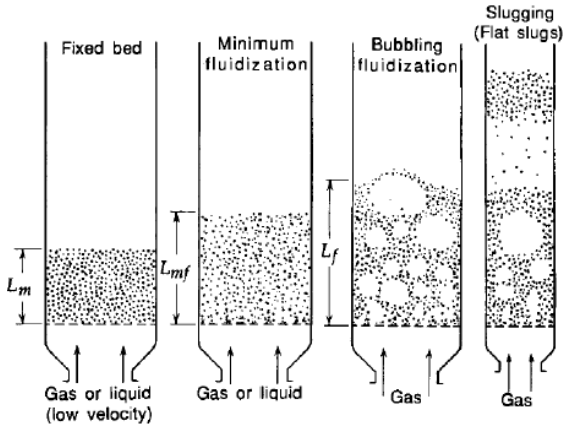

Figure 2.1: Schematic figure illustrating different regimes of a fluidized bed, source [8].

The critical superficial gas velocity, where the bed is fully suspended, is called minimum fluidization velocity($u_{mf}[\mathrm{m\,s^{-1}}]$). Superficial gas velocity is defined as volumetric flow of the gas divided by cross-sectional area as

$$u_s = \frac{Q}{A}) \quad [\mathrm{m\,s^{-1}}] \tag{2.1}$$

The onset of fluidization starts when the friction force exerted on the bed is equal to the weight of the particles. It can also be expressed with respect to the pressure drop as

$$\Delta P_{bed} = L_{mf}(1-\epsilon_{mf})(\rho_s - \rho_g)\frac{g}{g_c} \quad [9] \tag{2.2}$$

Where L_{mf} is the height of the bed, ϵ_{mf} the void fraction of the bed, $rho_s \mathrm{kg\,m^{-3}}$ density of fluidizing solids and rho_g density of the fluidizing gas. Lower g is the acceleration of gravity($9.81\ \mathrm{m\,s^{-2}}$) and g_c a conversion factor($1\ \mathrm{kg\,m\,N^{-1}\,s^{-2}}$). As the bed transforms from fixed bed to fluidized bed the pressure drop over the bed increases until minimum fluidization velocity is reached.
When u_{mf} is reached the bed becomes fluidized and the pressure drop stays relative constant, illustrated in figure 2.2.

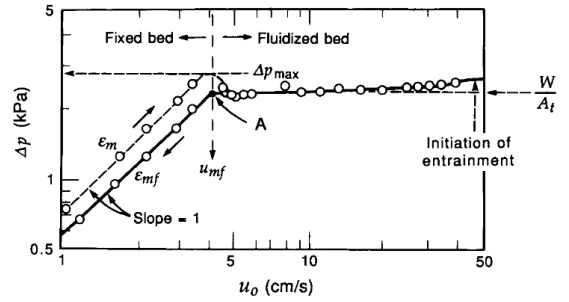

Figure 2.2: Pressure drop over bed Δp versus superficial gas velocity(u_o), where u_o is incrementally increased past u_{mf}.[10]

2.2 Packed-fluidized bed

One aspect of fluidized bed is the potential for reduced gas-solid mass transfer rate when the bed is fluidized and bubbles are present. Fluidized bed technology is more favorable for heat and mass transfer compared to other reactors, however the mass transfer can be improved. It has been showned by Jesper Aronsson et al to potentially be the rate limiting step in fuel conversion when using the fluidized solids as an oxygen carrier and gas as the fuel[1]. One disadvantage with bubbling fluidized bed is that the bulk of the fuel(gas) is located in the bubbles. The mass transfer occur at the boundary between gas and solids in a fluidized bed and therefore mass transfer decrease as bubbles grow in size [11]. If the bubble growth could be reduced in the fluidized bed system the mass transfer with respect to solid and gases would increase.

A novel approach to this problem is to introduce packing material distributed randomly in the reactor. The terms used for this are packed-fluidized or confined fluidized bed. The packing material is larger in diameter than the fluidized solid particles, The fluidiziation will occur in the void of packing material. The void of the packing material is measured by the void factor which is fraction of volume of packing over the total volume of the vessel. Sutherland et al. have shown that the pressure drop for confined bed is lower than for a bed without packings, given the same bed height [12].

Figure 2.3 shows a schematic picture of a confide fluidized bed. The packing material prevent the bubbles from coalescing and grow in size by effectively breaking down the bubbles as they hit the packing material. It has been shown by Aronsson et al that the mass transfer between gas and fluidizing solids increased by a factor of 1.9-3.8 when introducing packings to the reactor [13].

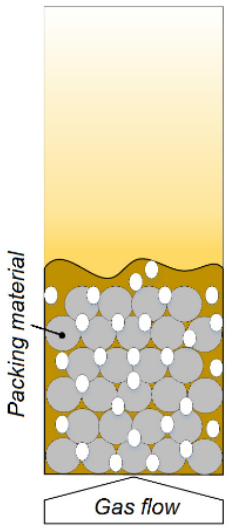

Figure 2.3: Schematic diagram of a packed fluidized bed. Grey circles represent packing material, white bubbles are the bubble phase and the brown color represent the gas emulsion phase. Source [14].

2.3 Plug flow and tracer method

Two common type of ideal reactor models in the chemical industry are continuous stirred tank reactor(CSTR) and plug flow reactor(PFR). CSTR are, as the name suggest, a tank with an inlet of reactants and a mixer that stirs such that the fluid is well mixed. Figure 2.4 shows a schematic diagram of a principal CSTR.

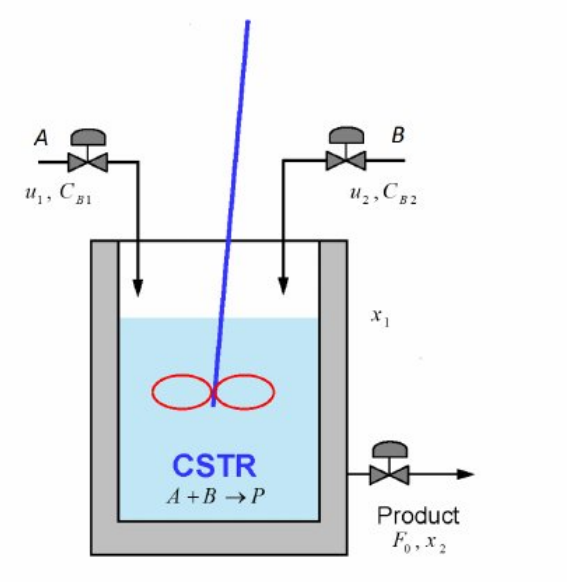

Figure 2.4: Schematic diagram of a continuous stirred tank reactor(CSTR) [15].

One disadvantage of the CSTR is the non-uniformal residence time distribution. Assume reactant A and B react to produce product P. As A + B $\longrightarrow$ P, some reactants will residence a short amount of time and some reactants much longer. This means that the number of residence time are infinite. CSTR are also limited by chemical equilibrium. Another disadvantage is that the concentration of reactant is constant throughout the reactor. This concentration is low because it is equal to the concentration of reactants at the outlet. Since the reaction rate is proportional to the reactants concentration the overall reaction rate is low, leading to a low production of the product.

To overcome these problems a reactor which utilize the concept of plug flow can be used. Figure 2.5 shows the setup for the experiments. Instead of having a tank reactor that is continuously stirred, the reactor takes the shape of a tube with an inlet and an outlet. The concentration of reactants will be low at the outlet and increase towards the inlet. To increase the residence time of a plug flow reactor the reactors length is simply increased.

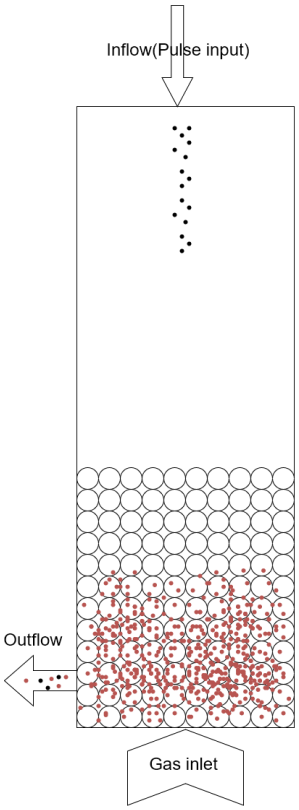

Figure 2.5: Schematic diagram of a reactor that utilize plug flow.

A plug flow reactor is an ideal tubular reactor, it's ideal since all the molecules move in a constant speed and are not mixed axially, they therefore move as a plug. Figure 2.6 shows a small volume element(i.e plug). The assumptions are that there is no axial mixing upstream or downstream of the plug and that the fluid is perfectly mixed radially. As the plug moves the residence time becomes a function of the plug position in the reactor. The residence time distribution looks like a pulse[16], see figure 2.6. For non-ideal plug flow, axial dispersion will most likely occur due to back mixing of the flow. Other deviation from ideal plug flow can be due to dead spots in the fluid in the tube, or channeling of fluid through the tube[17]. Dead spots occurs where there is stagnant flow, channeling when the fluid favors a certain path in the reactor.
If the flow from inflow towards outflow move as a plug and meet the gas flow coming from the bottom they will behave as counter-current flow with respect to each other. As mentioned in chapter 1 counter-current flow increases the mass transfer potential with respect to gas and solids. If gas is the fuel and fluidizing solid particles the oxidizer it would mean that almost fully reacted gas meets fully oxidized bed material.

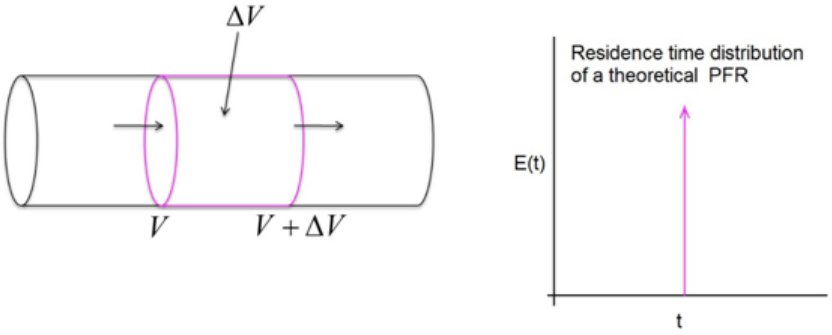

Figure 2.6: Schematic diagram of an ideal plug flow and its residence time, picture from [16].

The tracer input technique is a common technique for measuring the residence time distribution in reactors. One common method is the pulse input method where an inert tracer with known concentration is injected in the inlet of the reactor and its concentration is measured at the outlet. In an ideal plug flow reactor the measured signals would look identical. However due to axial dispersion they will not look identical in a real plug flow reactor. Figure 2.7 shows the general behavior of the tracer curve. The more dispersion that occurs due to affecting factors, the more spread out the tracer curve gets.

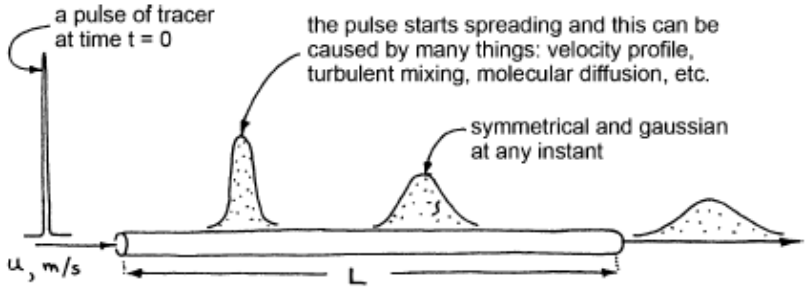

Figure 2.7: Tracer curve behavior close to plug flow, picture from [16].

A good tracer should have similar fluid dynamic properties as the bulk of the flow. Reynolds number can be used to ensure commonality between the tracer and the fluidized solid particles. Reynolds number describes the turbulence of a fluid or something behaving as a fluid(fluidized beds for example). Flow with high Reynolds number tend to be turbulent and flow with low Reynolds number tend to be laminar. Reynolds number is given by

$$Re = \frac{\rho u d_p}{\mu} \tag{2.3}$$

Where u[$\mathrm{m\,s^{-1}}$] is the velocity, ρ[$\mathrm{g\,cm^{-3}}$] the density and μ[Pa s] the dynamic viscosity. The inert and the tracer will experience the same superficial velocity and fluid viscosity, thus giving the equation

$$\frac{\rho_t}{\rho_s} = \frac{d_s}{d_t} \tag{2.4}$$

Which can be used to choose correct particle diameter for the inert tracer to match the behavior of the fluidising bed material. The flow will have a high degree of plug flow(close to ideality) if the pulse signal upstream looks like the pulse signal downstream. Real flow are not ideal and will have non-ideal plug flow, meaning the pulse signal downstream will look more stretched out compared to the one upstream, as figure 2.7 shows.

2.4 Dispersion model

To model and measure the degree of plug flow one can either use the tank in series model or the dispersion model. The dispersion model is characterized by the single dispersion number $\frac{D}{uL}$. The flows tendency to disperse can be due to turbulent mixing, molecular diffusion or laminar velocity profile[18]. The dispersion number can be used to get a quick glance of the spreading process of the tracer. Large number means there is a fast spreading of the tracer curve. A small number means slow spreading of the tracer curve. If $\frac{D}{uL} = 0$ there is no spread and the flow is ideal plug flow.

In this study the method used in example 3 page 67 from [18] will be used to calculate the dispersion number. The dispersion number is calculated using the one shot input method. It can be used since the pulse input is non-ideal the tracer curve for the inlet will have some variance. Referring to figure 2.7 it will look not like the first pulse but more like the second pulse. The dispersion number is therefore calculated as

$$\frac{D}{uL} = \frac{\Delta\sigma_\theta^2}{2} \tag{2.5}$$

where $\Delta\sigma_\theta^2$ is given by

$$\Delta\sigma_\theta^2 = \Delta\sigma^2 \frac{v}{V}^2 \tag{2.6}$$

where $\Delta\sigma^2$ is the difference between the variance of the inlet and outlet signals, $v[\mathrm{m\,s^{-1}}]$ is the superficial gas velocity and V is the free volume in the reactor between the inlet and outlet, it can be calculated as the length of reactor times the void factor. The variance of either inlet or outlet signal can be calculated using the following equation

$$\sigma^2 = \frac{\sum t_i^2 \cdot C_i}{\sum C_i} - \bar{t}^2 \tag{2.7}$$

If and only if the time interval is uniformly spaced. The mean of the curve, $\bar{t}$, can be calculated the same way if the time intervals are equal as

$$\bar{t} = \frac{\sum t_i \cdot C_i}{\sum C_i} \tag{2.8}$$

2.5 Bulk Density

Bulk density is given by

$$\rho = \sum_{i}^{n} \frac{m_i - m_{cup}}{n \cdot V_{cup}} \tag{2.9}$$

where i is each measured sample and n is the total number of samples.

3
Methods

In this chapter the methods, experimental setup and procedures used in the experiments are presented.

3.1 Experimental Setup

This section describes the experimental setup, physically and technically.

3.1.1 Reactor

The experiments were carried out in a cylindrical rector vessel made of Plexiglas with an inner diameter of 12 cm and a length of 1 m at laboratory-scale. Figure 3.1 shows the setup and the reactor excluding the top funnel where the tracer was poured in. Pressure sensors are located 2.1 7.6 and 13.2 cm from the bottom plate of the reactor. The air enters the reactor via a gas distribution plate located at the bottom of the reactor, air reaches the windbox before it flows through the plate. A pressure sensor is located in the windbox. Giving a total of 4 pressure sensors. Inductance sensors for the magnetic tracer are located 13.2 cm(outlet) and 47 cm(inlet) from the bottom distributor plate. The four pressure sensors measure pressure using Huba Control pressure transmitters which are digitized through a NiDAQ A/D converter and recorded in the program LabView™. The sensors have a sensitivity of ±500 mPa. The air that is fed to the system is regulated using a Bronkhorst mass flow meter. The output data from the two magnetic sensors were recorded and analyzed in LabView™on a different computer.

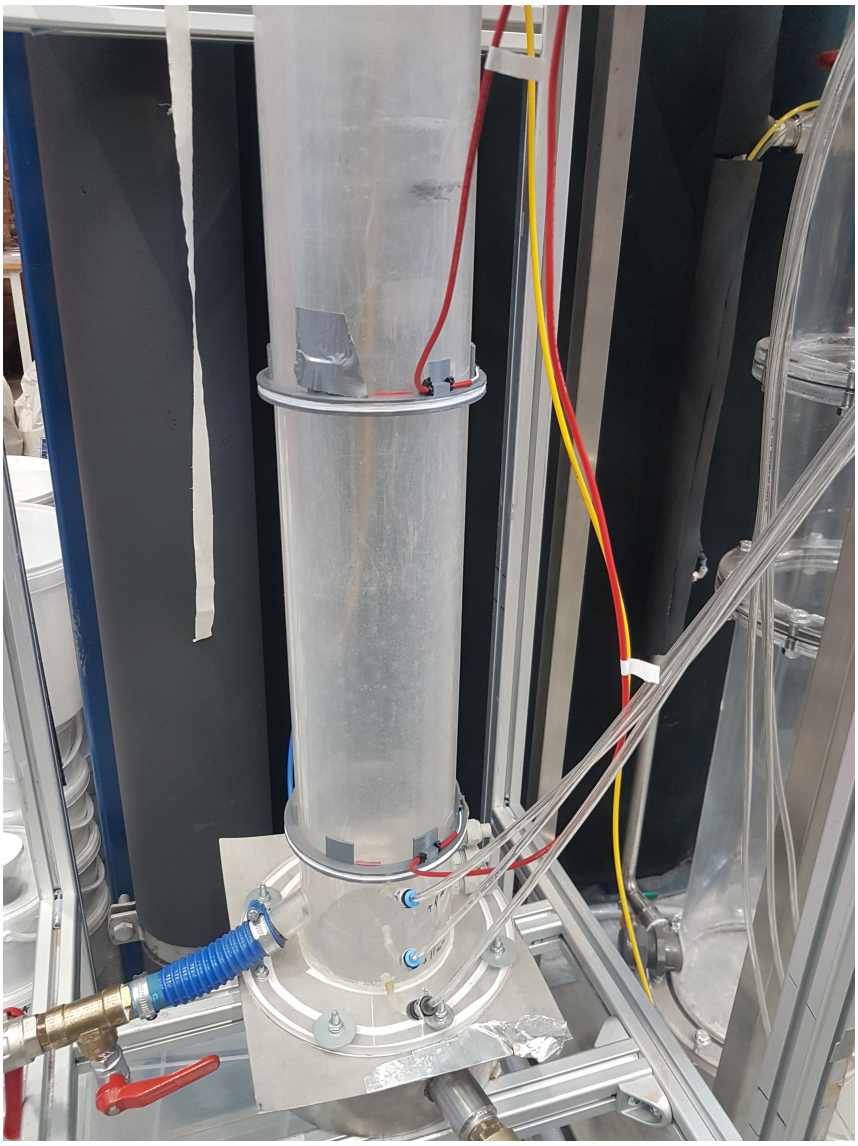

Figure 3.1: Picture of the reactor(excluding top funnel for input of tracer).

Figure 3.2 shows the full length of the reactor including the funnel for input of tracer. The outlet is more clearly seen in the left of the figure, this is where the manual sampling was taken.

Figure 3.2: Picture of the reactor,including top funnel for input of tracer.

Figure 3.3 shows a schematic picture of the reactor setup. Big white circles represent the packing material(ASB), the brown dots olivine sand(inert bed material) and the black dots the magnetic tracer. S1 and S2 are the two magnetic sensors used to measure the flow of tracer, this by giving a signal output proportional to the amount of tracer flowing through. S1 is the inflow sensor and S2 the outflow sensor placed at height above the plate mentioned earlier. Pressure sensors P1-P3 are placed at the positions mentioned earlier and $P_{windbox}$ the sensor that measure the pressure of the gas coming in to the reactor.
The downward arrow named sample at the outflow represent the valve used for collecting the manual samples during the experiment. olivine sand(brown dots) was fluidized by the air coming from the distributor at the bottom(gas inlet). The olivine sand doesn't give a signal output on the magnetic sensors(S1 and S2). The tracer, magnetite, was injected from the top via the funnel that can be seen in figure 3.2. The tracer(black dots) gave a signal output on the magnetic sensors.

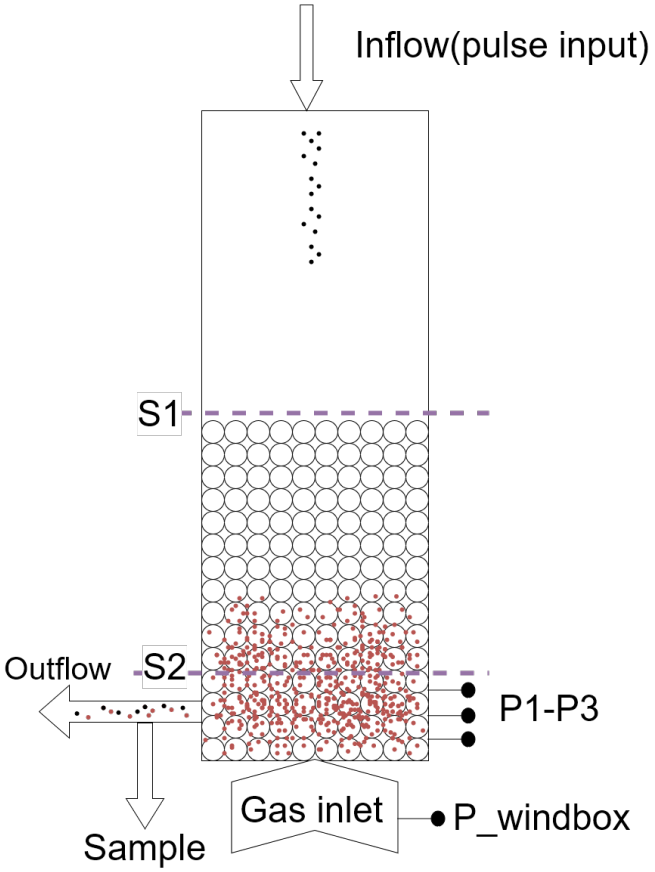

Figure 3.3: Schematic figure of the reactor. S1 is the position of the magnetic sensor for the inlet flow and S2 for the outlet. The arrow with the text sample is the valve presented in figure 3.1. Pressure sensors placed in the reactor are are $P_1 - P_3$ and $P_{windbox}$ pressure sensor for the fresh gas inlet.

3.2 Preparation

This section describes the preparation steps necessary in order to do the experiments.

3.2.1 Bed material

Olivine sand was used as the bed material. In order to be able to track sand particles inside the fluidized bed with magnetic sensors, magnetite was used as a tracer. Magnetite consist of iron oxide which is ferromagnetic, whilst having similar density as the olivine sand. An important parameter to consider is the properties of sand and magnetite such as their size and particle density. If these properties are similar then similar fluid dynamic behavior can be expected in the reactor. Thus, to be able to carry out the experiments correctly. Bulk densities of packing material,magnetite and sand particles had to be determined.

The materials were sieved using a sieving machine, see figure 3.5 for the machine

used and 3.4 for a sample of the sieves used. The sieves were stacked starting from bottom with a mesh of 90 µm followed by 125,150,180,212,250 and lastly 300 µm at the top. Top sieve was loaded with material, which was sieved for 25-30 minutes. The resulting fractions were stored in different containers with size that ranged between every mesh, and above and below the smallest and largest meshes.

Figure 3.4: Sample of sieves used, source [14]

Figure 3.5: Sieving Machine, brand Octagon, source [14]

3.2.2 Calculating bulk density and particle size for inert and tracer

For bed material and tracer, a density apparatus was used to calculate the bulk densities. The mass of the cup was $m_{cup} = 79.1$ g and the volume, $V_{cup} = 25.092\text{cm}^3$. The measures were repeated 10 times and averaged to get the bulk density, see table A.1 in appendix A for all measurements. Applying equation 2.9 yielded the following: Density for olivine sand to $\rho_{os} = 1.603\text{g}\,\text{cm}^{-3}$ and density for magnetic tracer, $\rho_{ms} = 2.603\text{g}\,\text{cm}^{-3}$. Equation 2.4 was applied giving a density ratio of $\frac{\rho_{ms}}{\rho_{os}} = 1.62$. The ratio was applied to diameter of olivine sand and tracer giving an olivine sand particle size of 250-300 µm and a particle size of the magnetic tracer of 180-212 µm.

3.2.3 Void factor of packing materials

The packing materials used for the confined fluidized bed are shown in figure 3.6 and figure 3.7.

Figure 3.6: Aluminum silicate balls (ASB) 25.4 mm in diameter, source [14]

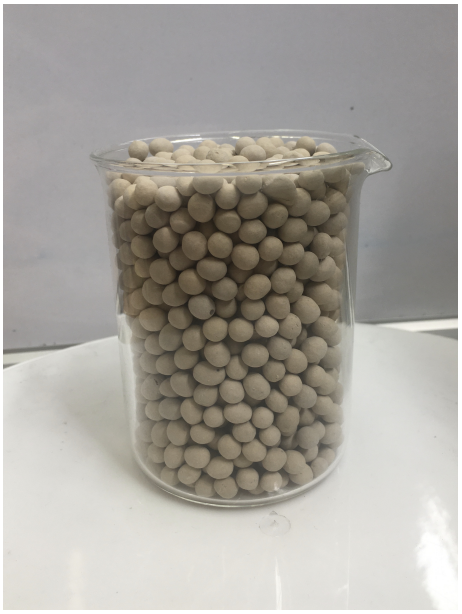

Figure 3.7: Aluminum silicate balls (ASB) 6.35 mm in diameter, source [14]

To be able to pour in the correct amount of sand for the experiments void factor of the packings needed to be determined. This was done using water displacement method. The void factor is given as $\epsilon = \frac{m_{void}}{m_{water}}$, where m_{water} is the mass of water filled into a container with known mass and volume. The water is removed and packing material is added to the same volume as before, after this water is added which fills the voidage surrounding the packing material. This new measurement is called m_{void} and all parameters for calculating void factor have been presented.

3.2.4 Packing and packing heights chosen

The packing material chosen for the experiments are ASB 25.4 mm and ASB 6.35 mm. Table 3.1 shows the parameters of the packings. The data is taken from [6].

Table 3.1: Density and void factor for packing material

Packing	bulk density $\rho_b$kg m^{-3}	void factor%
ASB 25.4 mm	1358.5	0.447
ASB 6.35 mm	1467.76	0.395

The packing and bed material were chosen to match a 2-2.5:1 ratio with a bed height of 20 and packing height of 50 cm. To calculate the weight of the packing the formula $A \cdot h \cdot \rho_{packing}$ was used. Where A is the cross sectional area, h the height of the stacked packing and $\rho_{packing}$ the density of the packing from table 3.1. In similar fashion the weight for the bed material olivine sand was calculated as $A \cdot h \cdot \rho_{sand} \cdot \epsilon$, where ϵ is the voidage factor from table 3.1 and ρ_{sand} the density of olivine sand calculated in section 3.2.2. For packing material ASB 25.4 mm mm, 8

kg was measured. 1.6 kg of bed material was measured to achieve 20 cm bed height. The amount of tracer material used for each experiment was set to 300 g. For the smaller packing material, ASB 6.35 mm, 1.4 kg of bed material and 6.7 kg of packing material were measured. When no packing material was used for the reactor(only a fluidized bed) 3.6 kg of sand was used. The total amount of olivine sand that was prepared and sieved was 3.8 kg.

3.2.5 Flow rate

An important parameter for the reactor to be similar to a plug flow reactor was to have matching inflow and outflow flow rates. Inflow flow rate was determined by pouring 1 kg of olivine sand with the inflow valve half opened and measure the time required for it to flow through completely. The time it took for the batch of sand to pour through was 9 seconds, giving a flow rate of 111.11 $\mathrm{kg\,s^{-1}}$. With the valve fully opened the flow rate was determined to be 222.22 $\mathrm{kg\,s^{-1}}$. The flow rate of the outflow was determined by averaging the weight of the manual samples taken from the sample valve. The outflow and sample valve both had the same diameter and the manual samples was taken at one seconds interval. The inflow and outflow valve were fully opened when experiments were running.

3.3 Experimental Procedure

This section describes the procedure of the experiment.

The experimental procedure step was as follow

1. The reactor was filled with packing material and bed material(olivine sand with size span 250-300 µm). 300 gram of tracer(magnetite of size span 180-212 µm) was put in the funnel at the top, inflow in figure 3.3. The remaining bed material was put in a bucket. This varied between packing material. ASB 25.4mm had 2.2 kg of remaining olivine sand, ASB 6.35 mm 2.4 and for no packing only 200 g remained. Both inflow and outflow valve were closed at this time, additionally the sample valve was closed.
2. The bed was fluidized at set superficial gas velocity of either 0.3 m/s(201 L/min) or 0.1 m/s(67 L/min) depending on the experiment. The pressure was recorded via pressure sensor at a sample rate of 50 Hz. Inductance response was recorded on a second computer with a sample rate of 10 Hz.
3. At the start of experiment, the inflow valve and outflow valve were rapidly opened. After the valves were opened, immediately the remaining bed material from the bucket was poured in to the funnel(inflow). To maintain a constant bed height. The bed height remained relative constant whilst the olivine sand from the bucket kept pouring in.
4. At the start of the experiment manual sampling was done at the outflow through the sample valve. The sample valve was opened every other second between 2 and 14 seconds from the time the inflow and outflow valves were opened(see figure 3.3). A total of seven samples were collected per experiment

in small plastic cups. The cups were weighted with sand and tracer in them and later on weighted with only tracer in them.

5. The experiment lasted until the bed material and tracer had exited the reactor and the reaming fluidized bed height was low enough to no longer give a signal for S2 or when the outflow was too low. The experiment was repeated three times for each packing and superficial gas velocity.

After the experiment was concluded the magnetite(tracer) was separated from the olivine sand(bed material). The sieving machine(figure 3.5) was loaded with sieves with meshes of size 300 and 180 µm. The machine sieved for 20-45 min. This yielded two samples, one with high concentration of olivine sand(non-magnetic) and one with high concentration of magnetic tracer.
The two samples were then separated further using a hand-held electromagnet. The electromagnet was turned on and tracer was picked up and put in an empty container, The process of picking up the tracer was repeated two to three times. The separation was not perfect and some olivine sand would still be present in the recycled magnetic tracer and some tracer would always be left in the olivine sand(bed material) container. The data was saved and processed using `MATLAB`. Dispersion numbers were calculated with the software program `MATLAB` using the equations given in section 2.4. Ratio of intensities were calculated as the difference between maximum peaks of inlet and outlet signals of the magnetic sensors.

Data from the pressure sensors were used to calculate the pressure drop over the bed. Pressure drop over the reactor was calculated as $P_{windbox} - P_x$, where $P_{windbox}$ is the pressure from incoming fluidizing air and x correspond to pressure sensors one to three.
Table 3.2 shows the packing material,gas velocity,packing and bed height chosen for each experiment, a total of 13 experiment were performed. Step 1 to 5 were done for each experiment. Experiment with low superficial gas velocity of 0.1 m/s and no packing material was not repeated due to no fluidization occurring for the setup.

Table 3.2: Experiments scheme.

Packing material	gas velocity($\mathrm{m\,s^{-1}}$)	Packing height(cm)	bed height(cm)
ASB 25.4 mm	0.3	50	20
	0.3	50	20
	0.3	50	20
	0.1	50	20
	0.1	50	20
	0.1	50	20
ASB 6.35 mm	0.3	50	20
	0.3	50	20
	0.3	50	20
No packing	0.3	-	20
	0.3	-	20
	0.3	-	20
	0.1	-	20

4

Results

In this chapter the results of the experiments are presented.

4.1 Packing material ASB 25.4 mm

Figure 4.1 shows the signal output from the inductance response for two experiments, one with ASB 25.4 mm and one with no packing in the reactor. The setups are identical apart from how much extra olivine sand(bed material) that was added after the pulse input(tracer), around 200 g of olivine sand was added for no packing and 2.2 kg was added for the setup with with ASB 25.4 mm. The superficial gas velocity in both experiments was set to 0.3 m/s or 201 L/min.

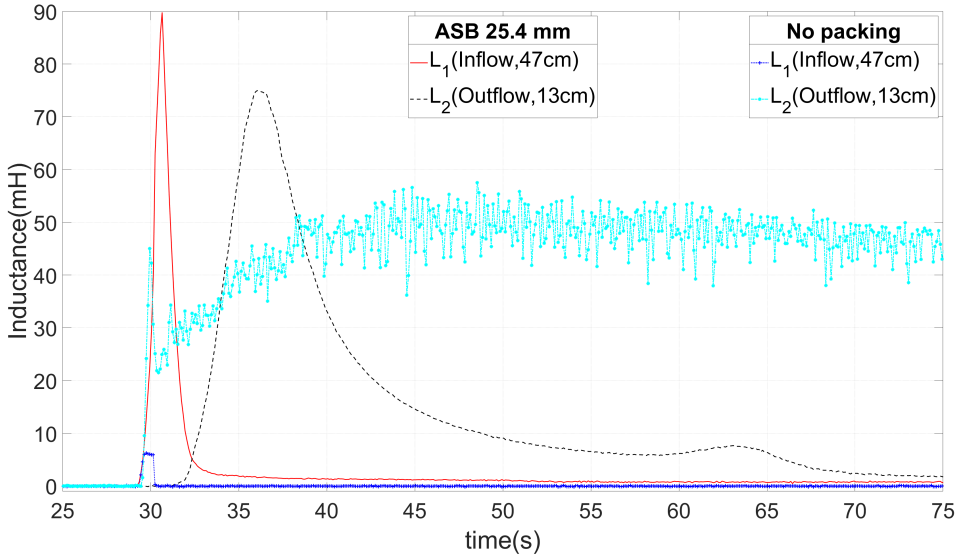

Figure 4.1: Mixing response from a pulse input of 300 g magnetic tracer in a confined bed and bed with no packing. The plot shows the inductance response of inlet and outlet sensors when a tracer is dispersed through the reactor for ASB 25.4 mm(red and black), compared with no packing(blue and cyan colored). The superficial gas velocity is 0.3 m/s(201 L/min), tracer size 180-212 µm and bed particle size 250-300 µm. The pressure data is sampled at 50 Hz and the inductance at 10 Hz. Magnetic sensors are placed 47 cm and 13 cm above the distributor plate.

The outlet signal is immediately visible for the case with no packing after introducing the tracer at 29 seconds. Thus the tracer is instantly mixed with the bed material.

For the setup with packing material ASB 25.4 mm the signals peak after 30.649 s for the inlet and 36.049 s, a six second delay between the two. This shows that the mixing between tracer and bed material is not instant and indicated that the packing material can facilitate a degree of plug flow with respect to solids. The non-ideal response indicates that there is axial mixing in the bed region, The outflow signal is stretching further in time compared to the narrow peak observed for inflow for the packing material. The observed noise in outflow signal for no packing could be due to slugging characterized by pulsating movement of the bed. The output signal from the sensors are sampled at 10 Hz and are not smoothed in post-process. The solid flux for the inlet for both setups were 19.649 $\mathrm{kg\,m^{-2}\,s^{-1}}$. The outlet solid flux was measured with manual sampling and averaged, see section 3.2.5. For no packing this resulted in an outflow flux of 2.9 $\mathrm{kg\,m^{-2}\,s^{-1}}$ and for packing material ASB 25.4 mm the outflow flux was 8.5 $\mathrm{kg\,m^{-2}\,s^{-1}}$.
Figure 4.2 shows the signal output from the inductance response for two experiment, ASB 25.4 mm and no packing in the reactor. The parameters are identical to those in figure 4.1, except for that the superficial gas velocity has been lowered to 0.1 m/s(67 L/min).

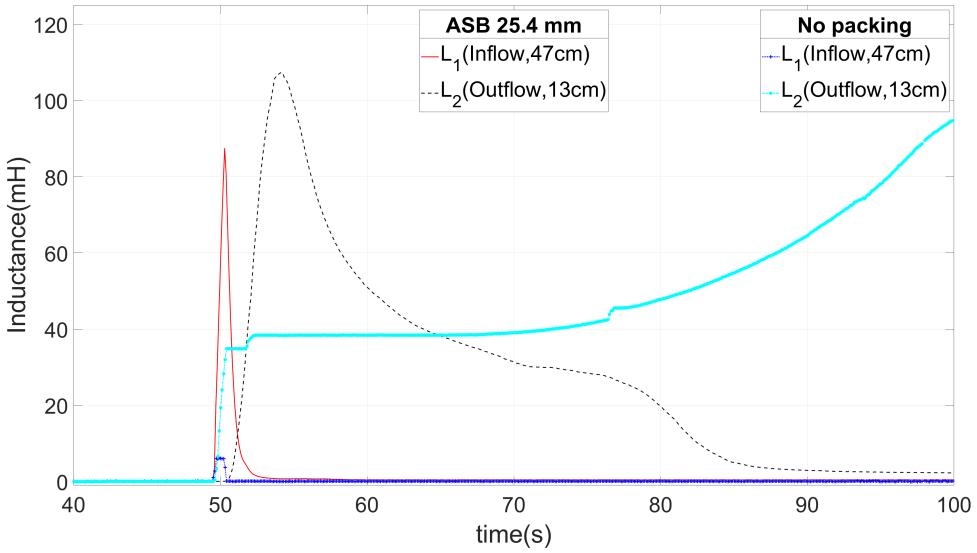

Figure 4.2: Mixing response from a pulse input of 300 g magnetic tracer in a confined bed and a bed with no packing. The superficial gas velocity is 0.1 m/s(67 L/min).

As can be seen in figure 4.1 the outlet signal for no packing is right after the inlet signal, indicating instant mixing of tracer and bed material. The inlet peak for the packing material is after 50.29 seconds and for the outlet 54.089 seconds, a 3.8 seconds delay between signal peaks. A degree of plug flow can be observed for packing material ASB 25.4 mm at superficial gas velocity of 0.1 m/s.

Figure 4.3 shows the pressure drop over the bed and the tracer curve for packing material ASB 25.4 mm in the bed at superficial gas velocity of 0.3 m/s. There is an inital drop in pressure drop when the tracer is introduced. As time progress the

pressure drop increases until another drop in pressure drop is observed in pressure sensor P_3, at the same time the pressure drop for sensors P_1 and P_2 levels out.

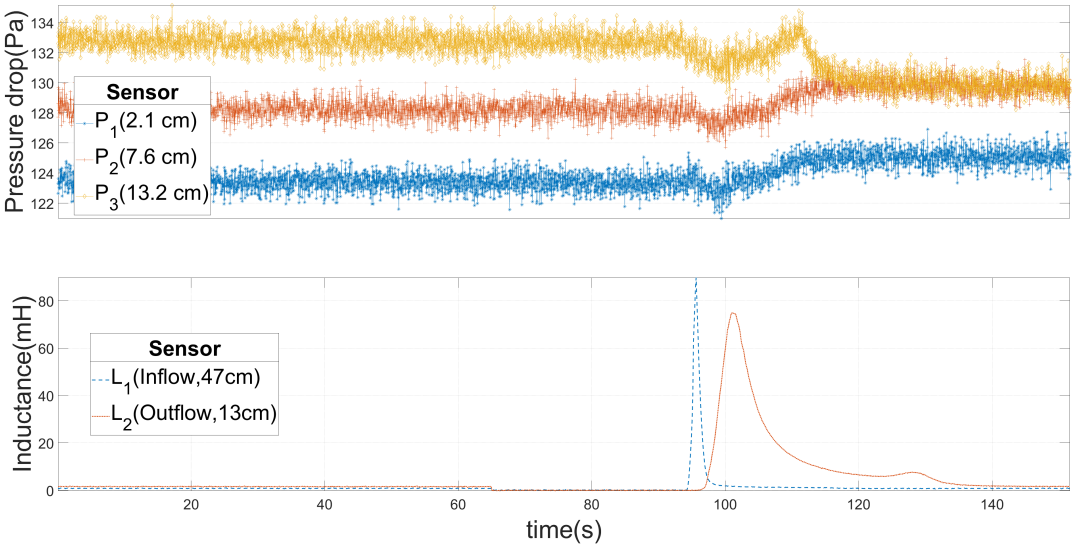

Figure 4.3: Mixing response from a pulse input of 300 g magnetic tracer with ASB 25.4 mm as packing material, superficial gas velocity is 0.3 m/s. upper graph shows the pressure drop over the bed at three set distances from the distributor plate. The bottom graph shows the tracer curve.

Figure 4.4 shows the pressure drop and the tracer curve when no packing is used. Higher pressure drop overall can be observed when no packing is used, max value for pressure sensor P_3 is 141.5 Pa for no packing and 135 Pa for ASB 25.4 mm. The decrease in pressure drop at the end of the experiment is due to bed material leaving the reactor through the outflow valve.

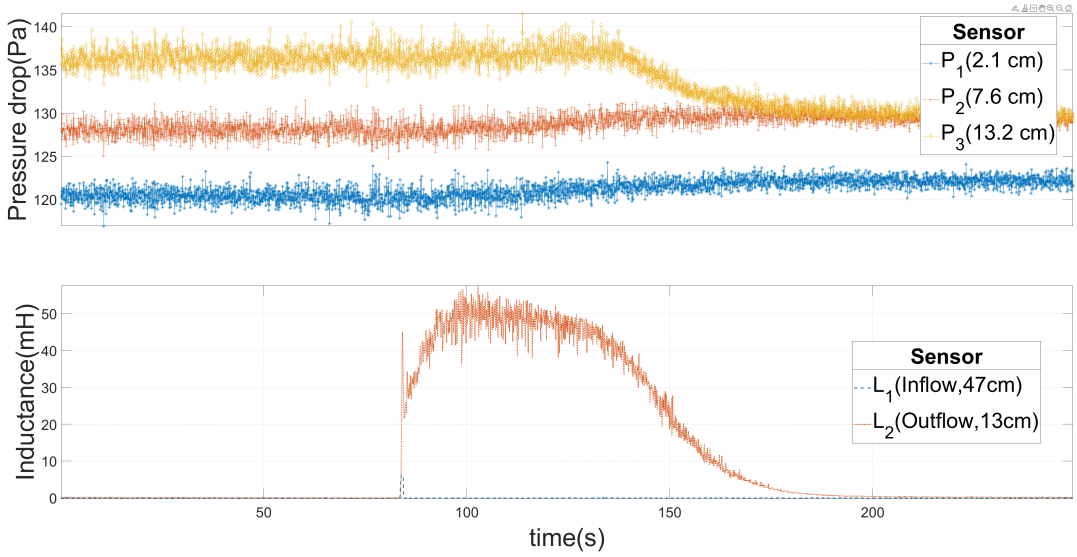

Figure 4.4: Mixing response from a pulse input of 300 g magnetic tracer with ASB 25.4 mm without packing material in the bed, superficial gas velocity is 0.3 m/s. upper graph shows the pressure drop over the bed at three set distances from the distributor plate. The bottom graph shows the tracer curve.

4.2 Manual Sampling

The tracer was also manually sampled, as previously mentioned in section 3.3, figure 4.5 shows the result from the experiments. Y-axis shows the amount of tracer collected from each sample, x-axis shows the time passed since start of experiment. The superficial gas velocity is 0.3 $\mathrm{m\,s^{-1}}$(201 L/min). Experiments were repeated to ensure consistency in the results. A degree of plug flow can be observed for experiment 1 for the packing material, but not for experiment 2 for the same packings given that the inlet signal is the same as in figure 4.1. No degree of plug flow is observed for the setup with no packing.

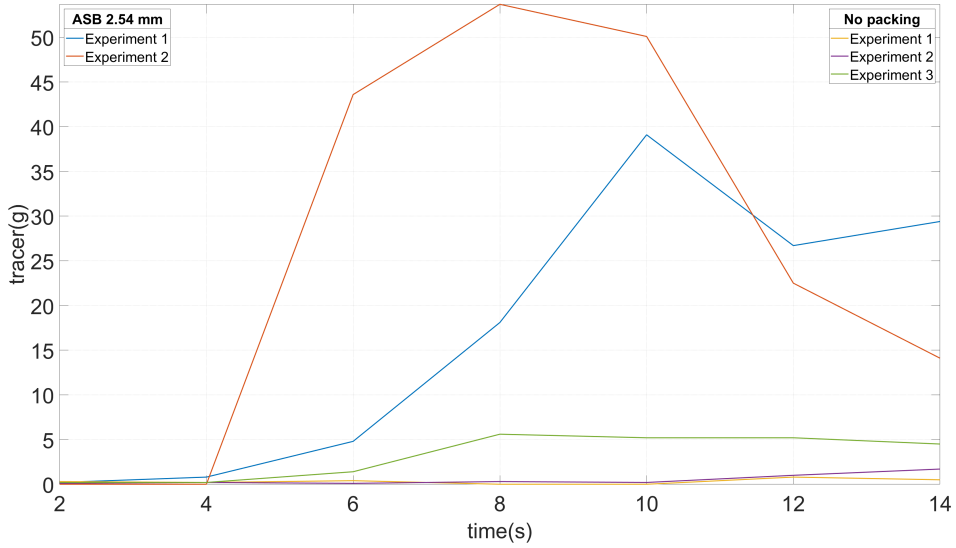

Figure 4.5: Mixing response from a pulse input of 300 g magnetic tracer in a confined bed and a bed with no packing. Tracer manually sampled at the outlet through a secondary valve(sample valve in figure 3.3).

4.3 Dispersion model

The dispersion number for the experiments were calculated with the software program `MATLAB` using the method presented in section 2.4. Table 4.1 shows key values calculated. The second column is superficial gas velocity, third column shows the ratio of intensities of output to input signals. Fourth and fifth column are the mean and variance for the outlet curve, which is concentration of magnetite over time for the outlet. Last column present the dispersion number. As stated in the section 2.4, a low value for D/uL indicates a high degree of plug flow and vice versa; a high number indicates a low degree of plug flow.
ASB 25.4 mm shows a lower dispersion number compared to bed without packing when the superficial gas velocity is 0.3 m/s. The median and mean values for ASB 25.4mm are 178.72 and 187.41. Without packing, median and mean rises to 2547.3 and 37290. With superficial gas velocity lowered to 0.1 m/s the dispersion numbers are lower. For ASB 25.4 mm the mean is 60.19 and with no packing in bed it's 49.4.

Table 4.1: Packing material and its corresponding value for superficial gas velocity,ratio of intensity, mean and variance of the inductance response curve and the dispersion number.

Packing material	u ($\mathrm{m\,s^{-1}}$)	$\frac{I_1}{I_2}$	$\bar{t}$	σ^2	$\frac{D}{uL}$
ASB 25.4 mm	0.3	1.040	225.08	150.75	129.44
		1.035	165.61	2414.4	178.72
		1.041	53.591	779.2	254.08
	0.1	1.046	75.142	499.01	36.10
		1.031	80.398	1874.8	97.09
		1.046	67.675	654.76	47.38
No packing	0.3	1.024	100.55	794.82	2547.3
		1.019	93.394	576.83	108,340
		1.023	80.168	518.26	982.2
	0.1	1.010	203.9	9361.2	49.415

The results from packing material ASB 6.35 mm is not presented since the experiment did not yield sufficient data to compare with other packing materials. At the start of the experiment the packing material ASB 6.35 mm started to flow out of the reactor, thus plugging the outlet. This resulted in the tracer and bed material not being able to escape the reactor and the bed material and tracer injected from the top through the funnel accumulated, thus giving a reading on the inlet magnetic sensor.

5
Discussion

This section the result and method are discussed, possible errors and limitations are presented.

5.1 Influence of packing on plug flow in fluidized bed

The aim of the study was to investigate the effect on the mixing response of pulse input during fluidisation. Comparing the ideal plug flow shown in chapter 2 with the ones observed for no packing and ASB 25.4 mm(figure 4.1 and 4.2), there is an observable effect of introducing packing material on the mixing response with respect to gas and solids.
With no packing in the reactor there is no delay between the input and output signals and the signal downstream do not match the signal upstream in any meaningful way. The introduction of packing material to the bed resulted in a delay between input and output signals and a sharper, albeit not equal, output signal closer resembling the input signal. This result indicates that there is high degree of plug flow when the packing material ASB 25.4 mm is introduced to the bed.
The broader peak of the output signal can be interpreted as back-mixing of tracer in the fluidized bed, indicating axial dispersion. Observing table 4.1, the dispersion number when no packing is used is 14 times bigger than ASB 25.4 mm at superficial gas velocity of 0.3 m/s. Bases on theses observations it can be concluded that there is no or extremely low degree of plug in the fluidized bed with no packings.

The pressure drop increases when tracer and remaining bed material are injected from the inflow valve. This can be observed in figure 4.3 and in figure 4.4. It is expected that pressure drop increases according to equation 2.2, since L_{mf} is increased. The pressure drop is slightly lower for ASB 25.4 mm compared to no packings. This could be due to less mass of fluidizing particles per unit of volume, since the packings occupy a part of the free volume.
Observing table 4.1, particularly the dispersion number, one can argue that the introduction of packing material ASB 25.4 mm shows potential for plug flow. It's not observable for the material when the gas velocity is 0.1 $\mathrm{m\,s^{-1}}$, however becomes clearly observable when the velocity is 0.3 $\mathrm{m\,s^{-1}}$.

Packing material ASB 6.35 mm did not perform as expected. The injected tracer and residual sand became stuck in the reactor and mixed with the original bed, producing a state of input only and no output. This could be prevented by employing a mesh

that is coarser than the olivine sand but much finer than the packing material, allowing the olivine sand to escape and flow through the outlet.

5.2 Error and limitations

There was a significant different in result for computerized compared to manual analysis. Figure 4.5 shows that the magnetic sensors have a considerably faster response time than the manual sampling, which may be due to the manual sampling not taking place in the same location as the magnetic sensors. Manual sampling displays a peak in tracer concentration at first and a subsequent drop, although it is less smooth than magnetic sensors, indicating a significant level of uncertainty in the tracer concentration. The data from the magnetic sensors are considered reliable for these experiments, but the data provided from the manual sampling is inconsistent and changes greatly between experiments. Manual sampling could be improved by sampling at a higher rate and for a longer period of time. Figure 4.5 illustrates the variation from manual sampling used for the experiments.

Pressure and inductance data are collected at different points in time and on two different computers. One improvement is to collect data from a single computer and match the time of injecting tracer to both pressure and inductance data.

Figure 4.1 shows a delayed small bump at the outlet around 130 seconds, this could be due to some clogging of tracer and bed material at the outlet or due to other factors This phenomena was observed in all three experiments for packing ASB 25.4mm at gas velocity 0.3 m/s. Due to the high cost of the tracer, it had to be recycled; even with sieving and electromagnets, some tracer remained in the remaining olivine sand. Perfect separation would require a different separation technique or a stronger electromagnet.

6
Conclusion

The following conclusions have been made from the experiments performed in this thesis:

- A high degree of plug flow is achieved when packing material ASB 25.4 mm is introduced to the reactor. No plug flow is observed for no packing material in the reactor. This demonstrates that the introduction of packing material to the reactor can facilitate counter-current flow with respect to solid and gas phases, which would allow for reactor design with performance better than thermodynamic equilibrium.
- The pressure drop decreases for packing material ASB 25.4 mm compared to without packing. The pressure drop increased when tracer and additional bed material was injected to the inflow.
- Packing material ASB 25.4 mm showed a degree of plug when introduced to the bed at superficial gas velocity of 0.3 m/s. It can be concluded from both methods that were used to measure the degree of plug flow.
- Low degree of plug flow and no improvement in counter-current flow patterns were seen with packing material ASB 6.35 mm. Proper investigation of the packing's performance can be facilitated by improving the experiments with a mesh at the outlet to prevent the packing material from clogging the outlet.

References

[1] Jesper Aronsson, Ewa Krymarys, Viktor Stenberg, Tobias Mattisson, Anders Lyngfelt, and Magnus Rydén. Improved gas–solids mass transfer in fluidized beds: Confined fluidization in chemical-looping combustion. *Energy & Fuels*, 33(5):4442–4453, 2019.

[2] David Pallarès. *Fluidized bed combustion – modeling and mixing*. PhD thesis, Chalmers University of Technology, 2008.

[3] SWCHING Technologies. Applications and markets, 2022.

[4] Valmet. Valmet CFB boiler, cited December 15, 2022.

[5] C. Gouedard, D. Picq, F. Launay, and P.-L. Carrette. Amine degradation in CO_2 capture. i. a review. *International Journal of Greenhouse Gas Control*, 10:244–270, 2012.

[6] Pablo Filiu Moreno. Characterisation of fluidization phenomena in packed-fluidized bed, 2021.

[7] S.D. Kim, C.G.J. Baker, and M.A. Bergougnou. Bubble characteristic in three phase fluidized beds. *Chemical Engineering Science*, 32(11):1299–1306, 1977.

[8] Daizo Kunii and Octave Levenspiel. Chapter 1 - introduction. In Daizo Kunii and Octave Levenspiel, editors, *Fluidization Engineering (Second Edition)*, pages 1–13. Butterworth-Heinemann, Boston, second edition edition, 1991.

[9] Daizo Kunii and Octave Levenspiel. Chapter 3 - fluidization and mapping of regimes. In Daizo Kunii and Octave Levenspiel, editors, *Fluidization Engineering (Second Edition)*, pages 61–94. Butterworth-Heinemann, Boston, second edition edition, 1991.

[10] Daizo Kunii and Octave Levenspiel. Chapter 3 - fluidization and mapping of regimes. In Daizo Kunii and Octave Levenspiel, editors, *Fluidization Engineering (Second Edition)*, pages 61–94. Butterworth-Heinemann, Boston, second edition edition, 1991.

[11] Daizo Kunii and Octave Levenspiel. Chapter 11 - particle-to-gas mass and heat transfer. In Daizo Kunii and Octave Levenspiel, editors, *Fluidization Engineering (Second Edition)*, pages 257–276. Butterworth-Heinemann, Boston, second edition edition, 1991.

[12] J. P. Sutherland, George Vassilatos, Hiroshi Kubota, and G. L. Osberg. The effect of packing on a fluidized bed. *AIChE Journal*, 9(4):437–441, 1963.

[13] Jesper Aronsson, David Pallarés, Magnus Rydén, and Anders Lyngfelt. Increasing gas–solids mass transfer in fluidized beds by application of confined fluidization—a feasibility study. *Applied Sciences*, 9(4), 2019.

[14] Mårten Bengtsson, Julia Cramstedt, Jesper Larsson, and Max Wassenius. Fluidisation characteristics of a confined fluidised bed - an evaluation of packing materialsl, 2020.

[15] Saeed Reza Tofighi, Farhad Bayat, and Farshad Merrikh-Bayat. Robust feedback linearization of an isothermal continuous stirred tank reactor: H mixed-sensitivity synthesis and dkiteration approaches. *Transactions of the Institute of Measurement and Control*, 39(3):344-351, 2017.

[16] Vapourtec. Plug flow reactor, 2022.

[17] Octave Levenspiel. *Chemical Reaction Engineering*. 3, illustrated, revised. John Wiley & Sons, 1998.

[18] Octave Levenspiel. *Tracer Technology*. Fluid Mechanics and Its Applications. Springer New York, NY, 2012.

A

Appendix 1

A.1 Bulk density calculations

For bed material and tracer a density apparatus was used to calculate the densities. The mass of the cup was m_{cup} = 79.1 g and the volume, V_{cup} = 25.092cm^3. The measures were carried out 10 times and averaged giving the table

Table A.1: Measured values for bulk density of olivin sand and magnetic tracer

Experiment	Olivine mass(g)	Tracer mass(g)
1	120.4	146.7
2	118.8	144.0
3	120.1	143.5
4	118.7	145.8
5	120.1	145.1
6	118.8	145.6
7	118.7	144.5
8	120.0	144.5
9	118.8	145.0
10	118.8	145.1

Table A.2: Measured values for bulk density of ASB 1"

Experiment	Mass(g)	Volume(cm^3)
1	305.5	250
2	444.0	325
3	282.5	250
4	219.9	200
5	293.9	250

A.2 MATLAB

```
1 clc, workspace, filebrowser, format shortg
```

```

% Short program for calculating disperson number, rate of intensity and
% plotting the plots for the thesis.


% Name of data to be imported.
strImportInductance = {'220315_102719_ASBbig1.txt', ...
    '220323_140627_data_ASBbig2.txt', ...
    '220330_164731_data_ASBbig3', ...
    '220406_133656_data_ASBbigLowVelo1', ...
    '220407_115225_data_ASBbigLowVelo2', ...
    '220407_153139_data_ASBbigLowVelo3', ...
    '220331_134509_data_ASBsmall1', ...
    '220404_123116_data_ASBsmall2', ...
    '220405_124031_data_ASBsmall3', ...
    '220324_101114_data_NoPacking1', ...
    '220324_141824_data_NoPacking2', ...
    '220328_151614_data_NoPacking3', ...
    '220408_141742_data_NoPackingLowVelo2'};

% Name of data to be imported.
strImportPressure = {'2022-03-15 10-32 ...
    s300t180ASB1p50b20g03AutoAndManual', ...
    '2022-03-29 14-53 s300t180ASB1p50b20g03AutoAndManual3', ...
    '2022-03-30 16-50 s300t180ASB1p50b20g03AutoAndManual3', ...
    '2022-04-07 11-50 s300t180ASB1p50b20g01AutoAndManual2', ...
    '2022-03-31 13-51 s300t180ASBsmallP50b20g03AutoAndManual1', ...
    '2022-04-05 12-46 s300t180ASBsmallP50b20g03AutoAndManual3', ...
    '2022-03-28 15-21 s300t180NoPackingB20g03AutoAndManual3', ...
    '2022-03-24 14-23 s300t180NoPackingB20g03AutoAndManual2', ...
    '2022-03-24 10-16 s300t180NoPackingB20g03AutoAndManual1', ...
    };

% Saving string. Important for saving plots.
strSave = {'bigASB1', 'bigASB2', 'bigASB3', 'bigASBlowVelo', ...
    'smallASB1', ...
    'smallASB2', 'NoPacking1', 'NoPacking2', 'NoPacking3'};


% Preallocation.
N = size(strImportInductance, 2);
M = size(strImportPressure, 2);
inductance = cell(1, N);
pressure = cell(1, M);


% Distribute inductance from txt-files to cells.
for i = 1:N
    inductance{i} = importfile(strImportInductance{i}, [1, inf]);
    inductance{i} = rmmissing(inductance{i}(:, 1:5));
end


% Distribute pressure from txt-files to cells.
for i = 1:M
```

```
55      pressure{i} = lvm_import(strImportPressure{i}, 0);
56  end
57
58  %% Calculating the mean and variance of the pulse response curve.
59
60  % Preallocation.
61  t_bar_inlet = zeros(1, N);
62  s_sqr_inlet = zeros(1, N);
63  t_bar_outlet = zeros(1, N);
64  s_sqr_outlet = zeros(1, N);
65
66
67  % Method Example 1 D/ul from a C curve.
68  for k = 1:N
69      t = inductance{k}.Times;
70      C = inductance{k}.L_A1 - inductance{k}.L_A1(1);
71      % Calcualate mean of the curve and variance of the curve.
72      t_bar_inlet(k) = sum(t.*C) / (sum(C));
73      s_sqr_inlet(k) = sum(t.^2.*C) / (sum(C)) - t_bar_inlet(k).^2;
74  end
75
76
77  for k = 1:N
78      t = inductance{k}.Times;
79      C = inductance{k}.L_A2 - inductance{k}.L_A2(1);
80
81      t_bar_outlet(k) = sum(t.*C) / (sum(C));
82      s_sqr_outlet(k) = sum(t.^2.*C) / (sum(C)) - -t_bar_outlet(k).^2;
83
84  end
85  % CORRECT!!!!
86  s_theta = s_sqr_outlet ./ (t_bar_outlet.^2);
87
88  V = 47 - 13; % Volume of container between the two sensors.
89  u = 100 * [repmat(0.3, 3, 1); repmat(0.1, 3, 1); repmat(0.3, 6, ...
        1); 0.1]';
90  % Superfical velocity in cm.
91  void = [repmat(0.4, 6, 1); repmat(0.4, 3, 1); ones(4, 1)]';
92  D = (s_sqr_outlet - s_sqr_inlet) .* (u ./ V).^2; % Dispersion ...
        coefficient.
93  DuL = D / 2;
94  disp(DuL')
95
96  % Calculate rate of intensity.
97  I_1 = zeros(1, N);
98  I_2 = zeros(1, N);
99  rI = zeros(1, N);
100 for k = 1:N
101     I_1(k) = max(inductance{k}.L_A1);
102     I_2(k) = max(inductance{k}.L_A2);
103     rI(k) = abs(I_1(k)/I_2(k));
104 end
105
106 %% plotting
107
108 % Plot Sizes.
```

```
109 legendFontsize = 36;
110 lineWidth = 1.8;
111 XaxisFontSize = 36;
112 YaxisFontSize = 36;
113 masterFontSize = 36;
114
115 % Names.
116 strLegend = {'L_1(Inflow,47cm)', 'L_2(Outflow,13cm)'};
117 legendTitle = {'Sensor'};
118 Xstring = {'time(s)'};
119 Ystring = {'Inductance(mH)'};
120 % Index for saving.
121 idx = [1, 2, 3, 5, 7, 8, 10, 11, 12];
122
123 for i = 1:length(idx)
124     k = idx(i);
125
126     plot(inductance{k}.Times, ...
        inductance{k}.L_A1-inductance{k}.L_A1(1), ...
127          'Color', 'r', 'LineWidth', lineWidth)
128     hold on
129     plot(inductance{k}.Times, ...
        inductance{k}.L_A2-inductance{k}.L_A2(1), ...
130          'Color', 'k', 'LineWidth', lineWidth)
131     hold off
132
133     % Set Y-axis
134
135     set(gca, 'FontSize', masterFontSize)
136     ylabel(Ystring, 'FontSize', ...
137         YaxisFontSize);
138     % Set X-axis
139     xlabel(Xstring, 'FontSize', ...
140         XaxisFontSize);
141
142     % Set legends.
143     l = legend('show');
144     l.TextColor = 'black';
145     l.FontAngle = 'italic';
146     l.FontSize = legendFontsize;
147     l.Title.String = legendTitle;
148     l.Title.Color = 'black';
149     legend(strLegend, 'FontSize', legendFontsize, 'FontAngle', ...
        'italic', ...
150          'Location', 'best');
151
152     % Other settings.
153     ax = gca;
154     grid on
155     axis tight
156     ax.GridLineStyle = ':';
157     ax.GridAlpha = 0.5;
158     % Save figure
159     set(gcf, 'WindowState', 'maximized');
160     newStr = join([strSave{i}, 'inductance.png']);
161     saveas(gcf, newStr)
```

```
162
163     pause(0.2)
164
165 end
166
167 %% Plot Pressure
168
169 % Names.
170 strLegend = {'P_1(2.1 cm)', 'P_2(7.6 cm)', 'P_3(13.2 cm)'};
171 legendTitle = {'Sensor'};
172 Xstring = {'time(s)'};
173 Ystring = {'Pressure drop(Pa)'};
174
175
176 for i = 1:length(idx)
177     k = idx(i);
178     t = pressure{i}.Segment1.data(:, 1);
179     P_W = pressure{i}.Segment1.data(:, 2);
180     P_1 = pressure{i}.Segment1.data(:, 3);
181     P_2 = pressure{i}.Segment1.data(:, 4);
182     P_3 = pressure{i}.Segment1.data(:, 5);
183
184     t_even = t(2:4:end);
185     P_1_even = P_W(2:4:end) - P_1(2:4:end);
186     P_2_even = P_W(2:4:end) - P_2(2:4:end);
187     P_3_even = P_W(2:4:end) - P_3(2:4:end);
188
189
190     plot(t_even, P_1_even)
191     hold on
192     plot(t_even, P_2_even)
193     plot(t_even, P_3_even)
194     hold off
195
196     % Set Y-axis
197
198     set(gca, 'FontSize', masterFontSize)
199     ylabel(Ystring, 'FontSize', ...
200         YaxisFontSize);
201     % Set X-axis
202     xlabel(Xstring, 'FontSize', ...
203         XaxisFontSize);
204
205     % Set legends.
206     l = legend('show');
207     l.TextColor = 'black';
208     l.FontAngle = 'italic';
209     l.FontSize = legendFontsize;
210     l.Title.String = legendTitle;
211     l.Title.Color = 'black';
212     legend(strLegend, 'FontSize', legendFontsize, 'FontAngle', ...
            'italic', ...
213          'Location', 'best');
214
215     % Other settings.
216     ax = gca;
```

```
217     grid on
218     axis tight
219     ax.GridLineStyle = ':';
220     ax.GridAlpha = 0.5;
221     % Save figure
222     set(gcf, 'WindowState', 'maximized');
223     newStr = join([strSave{i}, 'pressure.png']);
224     saveas(gcf, newStr)
225 
226     pause(0.2)
227 
228 
229 end
230 
231 %% Compare ASB and no packing
232 clc
233 % Plot Sizes.
234 legendFontsize = 24;
235 lineWidth = 1.8;
236 XaxisFontSize = 36;
237 YaxisFontSize = 36;
238 masterFontSize = 36;
239 
240 % Names.
241 strLegend = {'L_1(Inflow,47cm)', 'L_2(Outflow,13cm)'};
242 legendTitle1 = {'ASB 25.4 mm'};
243 legendTitle2 = {'No packing'};
244 Xstring = {'time(s)'};
245 Ystring = {'Inductance(mH)'};
246 
247 % strImportInductance = {'220315_102719_ASBbig1.txt', ...
248 %     '220323_140627_data_ASBbig2.txt', ...
249 %     '220330_164731_data_ASBbig3', ...
250 %     '220406_133656_data_ASBbigLowVelo1', ...
251 %     '220407_115225_data_ASBbigLowVelo2', ...
252 %     '220407_153139_data_ASBbigLowVelo3', ...
253 %     '220331_134509_data_ASBsmall1', ...
254 %     '220404_123116_data_ASBsmall2', ...
255 %     '220405_124031_data_ASBsmall3', ...
256 %     '220324_101114_data_NoPacking1', ...
257 %     '220324_141824_data_NoPacking2', ...
258 %     '220328_151614_data_NoPacking3', ...
259 %     '220408_141742_data_NoPackingLowVelo2'};
260 
261 % ASB 25.4 mm
262 a = 3;
263 b = 12;
264 shiftXstart2 = 53.5;
265 
266 % ASB 6.35 mm
267 % a = 2;
268 % b = 10;
269 % shiftXstart = 67.8;
270 
271 y1 = plot(inductance{a}.Times+shiftXstart, ...
        inductance{a}.L_A1-inductance{a}.L_A1(1), ...
```

```
272     'Color', 'r', 'LineWidth', lineWidth);
273 hold on
274 y2 = plot(inductance{a}.Times+shiftXstart, ...
        inductance{a}.L_A2-inductance{a}.L_A2(1), ...
275     'Color', 'k', 'LineWidth', lineWidth);
276
277 h1 = plot(inductance{b}.Times+shiftXstart2, ...
        inductance{b}.L_A1-inductance{b}.L_A1(1), ...
278     'Color', 'b', 'LineWidth', lineWidth);
279
280 h2 = plot(inductance{b}.Times+shiftXstart2, ...
        inductance{b}.L_A2-inductance{b}.L_A2(1), ...
281     'Color', 'c', 'LineWidth', lineWidth);
282
283
284 % Set Y-axis
285
286 set(gca, 'FontSize', masterFontSize)
287 ylabel(Ystring, 'FontSize', ...
288     YaxisFontSize);
289 % Set X-axis
290 xlabel(Xstring, 'FontSize', ...
291     XaxisFontSize);
292 % Other settings.
293 ax = gca;
294 grid on
295 % axis([96, 100, -5, 40]) % ASB 25.4 mm
296 axis([80, 150, -1, 90]) % ASB 25.4 mm
297 % axis([30, 290, 0, 50]) % ASB 6.35mm
298 % axis tight
299 ax.GridLineStyle = ':';
300 ax.GridAlpha = 0.5;
301 % Set legends for first plot
302 % l = legend('show');
303 % l.TextColor = 'black';
304 % l.FontAngle = 'italic';
305 % l.FontSize = legendFontsize;
306 % l.Title.String = legendTitle1;
307 % l.Title.Color = 'black';
308 % legend(strLegend, 'FontSize', legendFontsize, 'FontAngle', ...
        'italic', ...
309 %     'Location', 'best');
310 % lgd1 = legend([y1 y2],strLegend, 'Location', 'northeast');
311 % lgd2 = legend([h1 h2], strLegend, 'Location', 'northwest');
312
313
314 leg1 = legend([y1,y2], strLegend, 'Location', 'north');
315 set(leg1, 'FontSize', legendFontsize);
316 l = legend('show');
317 l.Title.String = legendTitle1;
318 ax2=axes('position',get(gca,'position'),'visible','off');
319 leg2 = legend(ax2,[h1,h2], strLegend, 'Location', 'northeast');
320 l = legend('show');
321 l.Title.String = legendTitle2;
322 set(leg2, 'FontSize', legendFontsize);
323
```

```
324
325
326
327 % Save figure
328 set(gcf, 'WindowState', 'maximized');
329 newStr = join(['CompareBigASB', 'inductance.png']);
330 saveas(gcf, newStr)
331
332 pause(0.2)
333 hold off
334
335 %% Small aSb
336
337 clc
338 % Plot Sizes.
339 legendFontsize = 24;
340 lineWidth = 1.8;
341 XaxisFontSize = 36;
342 YaxisFontSize = 36;
343 masterFontSize = 36;
344
345 % Names.
346 strLegend = {'L_1(Inflow,47cm)', 'L_2(Outflow,13cm)'};
347 legendTitle1 = {'ASB 6.35 mm'};
348 legendTitle2 = {'No packing'};
349 Xstring = {'time(s)'};
350 Ystring = {'Inductance(mH)'};
351
352 % strImportInductance = {'220315_102719_ASBbig1.txt', ...
353 %     '220323_140627_data_ASBbig2.txt', ...
354 %     '220330_164731_data_ASBbig3', ...
355 %     '220406_133656_data_ASBbigLowVelo1', ...
356 %     '220407_115225_data_ASBbigLowVelo2', ...
357 %     '220407_153139_data_ASBbigLowVelo3', ...
358 %     '220331_134509_data_ASBsmall1', ...
359 %     '220404_123116_data_ASBsmall2', ...
360 %     '220405_124031_data_ASBsmall3', ...
361 %     '220324_101114_data_NoPacking1', ...
362 %     '220324_141824_data_NoPacking2', ...
363 %     '220328_151614_data_NoPacking3', ...
364 %     '220408_141742_data_NoPackingLowVelo2'};
365
366 % ASB 25.4 mm
367 a = 8;
368 b = 11;
369 shiftXstart2 = 41;
370
371 % ASB 6.35 mm
372 % a = 2;
373 % b = 10;
374 % shiftXstart = 67.8;
375
376 y1 = plot(inductance{a}.Times+shiftXstart, ...
       inductance{a}.L_A1-inductance{a}.L_A1(1), ...
377     'Color', 'r', 'LineWidth', lineWidth);
378 hold on
```

```
379 y2 = plot(inductance{a}.Times+shiftXstart, ...
        inductance{a}.L_A2-inductance{a}.L_A2(1), ...
380      'Color', 'k', 'LineWidth', lineWidth);
381
382 h1 = plot(inductance{b}.Times+shiftXstart2, ...
        inductance{b}.L_A1-inductance{b}.L_A1(1), ...
383      'Color', 'b', 'LineWidth', lineWidth);
384
385 h2 = plot(inductance{b}.Times+shiftXstart2, ...
        inductance{b}.L_A2-inductance{b}.L_A2(1), ...
386      'Color', 'c', 'LineWidth', lineWidth);
387
388
389 % Set Y-axis
390
391 set(gca, 'FontSize', masterFontSize)
392 ylabel(Ystring, 'FontSize', ...
393     YaxisFontSize);
394 % Set X-axis
395 xlabel(Xstring, 'FontSize', ...
396     XaxisFontSize);
397 % Other settings.
398 ax = gca;
399 grid on
400 axis([100,180, -1, 70]) % ASB 25.4 mm
401 % axis([30, 290, 0, 50]) % ASB 6.35mm
402 % axis tight
403 ax.GridLineStyle = ':';
404 ax.GridAlpha = 0.5;
405 % Set legends for first plot
406 % l = legend('show');
407 % l.TextColor = 'black';
408 % l.FontAngle = 'italic';
409 % l.FontSize = legendFontsize;
410 % l.Title.String = legendTitle1;
411 % l.Title.Color = 'black';
412 % legend(strLegend, 'FontSize', legendFontsize, 'FontAngle', ...
        'italic', ...
413 %     'Location', 'best');
414 % lgd1 = legend([y1 y2],strLegend, 'Location', 'northeast');
415 % lgd2 = legend([h1 h2], strLegend, 'Location', 'northwest');
416
417
418 leg1 = legend([y1,y2], strLegend, 'Location', 'north');
419 set(leg1, 'FontSize', legendFontsize);
420 l = legend('show');
421 l.Title.String = legendTitle1;
422 ax2=axes('position',get(gca,'position'),'visible','off');
423 leg2 = legend(ax2,[h1,h2], strLegend, 'Location', 'northeast');
424 l = legend('show');
425 l.Title.String = legendTitle2;
426 set(leg2, 'FontSize', legendFontsize);
427
428
429
430
```

```
% Save figure
set(gcf, 'WindowState', 'maximized');
newStr = join(['CompareSmallASB', 'inductance.png']);
saveas(gcf, newStr)

pause(0.2)
hold off
```

DEPARTMENT OF SPACE, EARTH AND ENVIRONMENT
CHALMERS UNIVERSITY OF TECHNOLOGY
Gothenburg, Sweden
www.chalmers.se

CHALMERS
UNIVERSITY OF TECHNOLOGY